Journal of Molecular Graphics and Modelling 40 (2013) 131–139

Contents lists available at SciVerse ScienceDirect

Journal of Molecular Graphics and Modelling

journal homepage: www.elsevier.com/locate/JMGM

Computer modeling on the tautomerization of sulbactam intermediate in SHV-1 β-lactamases: E166A mutant vs. wild type

Rui Li[a], Yeng-Tseng Wang[b], Cheng-Lung Chen[c,*]

[a] Department of Chemistry, Liaocheng University, Liaocheng 252059, Shandong, China
[b] National Center for High-Performance Computing, Hsin-Shi, Tainan 74147, Taiwan, ROC
[c] Department of Chemistry, National Sun Yat-Sen University, Kaohsiung 80424, Taiwan, ROC

ARTICLE INFO

Article history:
Accepted 10 December 2012
Available online 31 December 2012

Keywords:
Molecular dynamics simulations
Density functional theory
Tautomerization
Proton transfer
β-Lactamases

ABSTRACT

We present a theoretical study for the tautomerization of sulbactam intermediates in different SHV-1 β-lactamases: E166A and wild-type (WT). Molecular dynamics (MD) simulations were employed and hydrogen bonds network around active site was found different between the WT and E166A acyl-enzymes. In E166A, Asn170 restricts the C5—C6 bond rotation, thus stabilizes the dihedral angle N4—C5—C6—C7 of imine to a trans conformation. The DFT calculations (B3LYP/6-31+G* and B3LYP/6-31++G**) were performed on tautomerization reactions. Two mechanisms including direct and stepwise proton transfer reactions were proposed based on the MD results. In E166A, the substrate carboxyl group acts as a relay station which assists the proton transfer with a very low energy barrier. However, in WT, such stepwise mechanism is difficult to proceed because of the large separation between C6 and substrate carboxyl group. Our results explain why E166A SHV-1 β-lactamases forms greater population of trans-enamine than WT.

1. Introduction

β-Lactam antibiotics are clinically important in the treatment of infectious diseases due to their ability to inhibit peptidoglycan synthesis in bacteria and their low toxicity [1]. However, the appearance of β-lactamases presents a serious and growing threat to the efficacy of antibacterial chemotherapy thus it becomes a major challenge to human health [2]. β-Lactamase enzymes have been divided into four classes (A–D) on the basis of the activity site differences [3]. Among the four β-lactamase classes, the class A enzymes are the most frequently encountered in the clinic [4]. One of the most successful strategies to overcome β-lactamase resistance is to use β-lactamase inhibitors. Currently, three β-lactamase inhibitors are available for clinical use: tazobactam, sulbactam, and clavulanic acid. Their mechanisms of action have been studied extensively [5–14] and a common mechanism has been proposed: in the first step, the catalytic serine (Ser70) attacks the carbonyl carbon of the β-lactam ring, forming an acyl-enzyme intermediate (AEI) with β-lactam ring opening. In the second step, AEI undergoes further reaction to generate a linear imine intermediate with five-member ring opening. Lastly, a series of proton transfers can occur and the imine AEI tautomerizes to yield a more stable cis- or trans-enamine intermediate thus providing transient inhibition (Fig. 1).

Experimental studies have utilized the deacylation deficient enzyme (E166A) to trap its acyl-enzyme intermediates for crystallographic analysis [8,10,11,14]. Previous studies have indicated that Glu166 acted as general base which was essential for deacylation of AEI. In E166A, the catalytic Glu166 was replaced by Ala166 and thus prevented regeneration of active enzyme. The accumulation of acyl-enzyme intermediates facilitates trapping AEI for crystallographic analysis.

Padayatti et al. have examined the mechanism of inhibition of E166A SHV-1 β-lactamase by sulbactam using Raman microscopy and X-ray crystallography [10]. The high resolution crystal structures of sulbactam bound to the E166A β-lactamase had been obtained. The sulbactam intermediate was observed in the trans-enamine form and named "waiting room" intermediate that is important for effective β-lactamase inhibition. Kalp et al. also reported the Raman microscope study for sulbactam bound to SHV-1 [15]. Their results showed that the trans-enamine population appeared to predominate for E166A. However, with the wild type (WT) enzyme, it was observed that sulbactam formed a mixture of trans-enamine and two labile species, the cisenamine and imine. This result suggests laboratory mutants, such as E166A, may not be a reliable basis for structure-based drug design.

However, the reason why WT and E166A SHV-1 show different AEI population is still under discussion and further studies on the mechanism of tautomerization from imine to enamine are certainly

* Corresponding author. Tel.: +886 07 5253935; fax: +886 07 5253909.
E-mail address: chen1@mail.nsysu.edu.tw (C.-L. Chen).

1093-3263/$ – see front matter © 2012 Elsevier Inc. All rights reserved.
http://dx.doi.org/10.1016/j.jmgm.2012.12.002

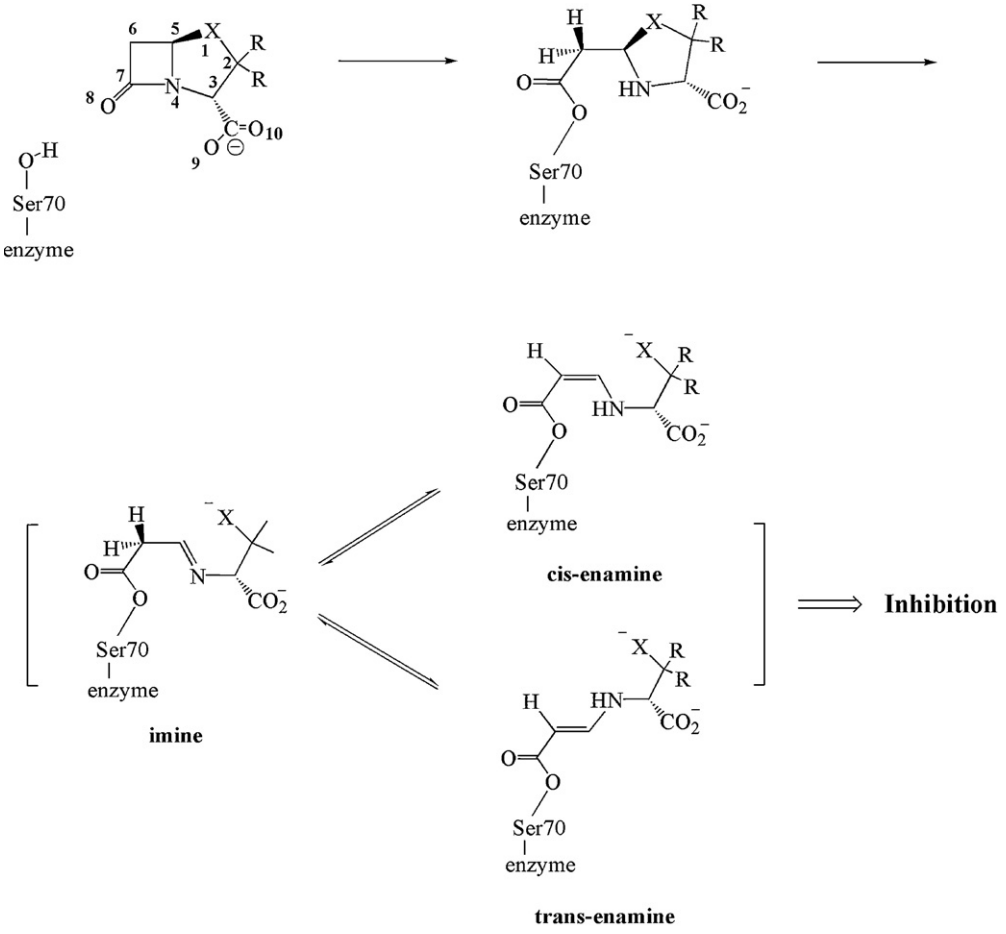

Fig. 1. Proposed reaction scheme for inhibitors with class A β-lactamases.

required. Herein, we explored the potential conformations of imine AEI in WT and E166A respectively by carrying out MD simulations. Along the simulations, we checked the structural and dynamical changes of the imine AEI in different protein environments, and characterized the specific role of the key residues in anchoring the substrate. Besides, quantum mechanical density functional theory (DFT) calculations were performed for the mechanistic study on the tautomerization of linear intermediates. Our studies reveal imine AEI is a key intermediate, and its dynamic behaviors are different in WT and E166A, which affect the population of intermediates. All of these theoretical results will be potentially useful in the design of improved mechanism-based β-lactamase inhibitors.

2. Models and methods

Two systems were performed MD simulations in the current study, namely **imine_E166A** and **imine_WT** respectively. The initial coordinates for sulbactam bound to E166A SHV-1 were taken from the crystal structural data 2A3U [10] of the Protein Data Bank (PDB). Based on this structure, the imine configuration of sulbactam (**SUL**) bound to Ser70 was constructed (**imine_E166A**). Then, the imine structure of sulbactam bound to WT SHV-1 (**imine_WT)** was constructed by mutating the Ala166 residue in the 2A3U structure into a Glutamic acid residue using Discovery Studio 2.5 package of programs.

In both of the computed system, the crystal waters from the PDB structure were conserved, and the complex was surrounded by a periodic box (79.83 Å × 69.36 Å × 64.85 Å) containing TIP3P water molecules. The total number of water molecules was 9343, and the closest distance between any atom of protein and the edge of the periodic box is 10 Å. Na^+ counterions (one for **imine_E166A** and two for **imine_WT**) were placed by LEaP module of the AMBER 10 computational program package [16] to neutralize the system. Atomic charges for substrates and substrate-bound Ser70 were determined using RESP module. The electrostatic potential at points selected according to the Merz–Shigh–Kollman scheme for use in the RESP module was calculated at the RHF/6-31G** level by Gaussian 03 software program [17]. Force field parameters for the protein were assigned from the "parm99" set of parameters [18], while the parameters of substrates were obtained from the "gaff" parameters [19] within AMBER 10. Previous studies [20–22] suggest that such a force field was appropriate for β-lactam compounds. Solvent molecules and counterions were initially relaxed by means of energy minimizations. Then the full system was minimized to remove bad contacts in the initial geometry. The steepest descent method followed by conjugate gradient method was performed for the minimization process. After that, MD simulation with position-restrain, which restrained the atomic positions of the macromolecule while allowed the solvent molecules to move, was carried out for 20 ps. Finally, a 20 ns MD simulation was performed for the system. In the MD process, the SHAKE procedure [23] was applied to constrain all bonds involving hydrogen atoms. The Langevin dynamics [24] was used to control the temperature at 300 K using a collision frequency of 1.0 ps^{-1}. Isotropic position scaling was used to maintain the pressure at 1 atm and a relaxation time of 2 ps was used. Periodic boundary conditions were used with a particle mesh Ewald (PME) [25] implementation of the Ewald sum for the description of long-range electrostatic interactions. A cut-off of 10 Å was used for other nonbonded interactions.

In order to study the proton transfer process, we carried out DFT quantum mechanical (QM) calculations. The initial coordinates of imine AEI reactant were obtained from the average structure of MD simulation. Subsequently the geometries of reactants, transition states, and products were fully optimized at the B3LYP/6-31+G* and B3LYP/6-31++G** level respectively [26,27]. These methods are suitable for current systems, and they have been used to study acylation mechanism of β-lactamase in previous studies [28–31]. Normal frequency analysis was performed on all structures to confirm that reactants, and products have no imaginary frequencies and transition states have only one imaginary frequency. Solvent effects were considered via polarizable continuum model (PCM) [32], and the radii type for the PCM calculation is Universal Force Field (UFF). Water was used as solvent, through the value 78.39 for the dielectric constant in the PCM calculations. All energies were calculated including zero-point vibration energy (ZPE). Intrinsic Reaction Coordinate (IRC) [33] calculations were carried out to confirm the reaction paths on the potential energy surface connecting the different reactants, transition states and products. All QM calculations were carried out using the Gaussian03 package of programs [17].

3. Results and discussion

3.1. Hydrogen bond network in active site

To judge the convergence of the MD simulations, the root-mean-square deviation (rmsd) of the obtained MD trajectories were calculated. Rmsd time series indicated that the simulations were well equilibrated after about 700 ps (Figure S1 in Supplementary material). We have checked the hydrogen bond network of the two systems respectively by analyzing MD trajectories and found there are some differences between these two systems. The typical snapshots of the active site region and schematic representations of the most important interresidue contacts observed during the MD simulations are shown in Fig. 2. The mean values for the significant interatomic distances between heavy atoms are summarized in Table 1.

Table 1
Important average distance (in Å) in active site.

System	**Imine_E166A**	**Imine_WT**
Nδ@Asn170···Oε1@Glu166		3.08 (0.3211)[a]
Oε2@Glu166···Nζ@Lys73		2.78 (0.1483)
Nδ@Asn170···O9@SUL	2.93 (0.2057)	5.96 (0.5532)
O10@SUL···Nδ@Asn132	3.15 (0.2987)	3.18 (0.2658)
Nζ@Lys73···O@Ser130	2.86 (0.1753)	2.88 (0.2015)
Oγ@Ser70···Nζ@Lys73	4.74 (0.5210)	3.25 (0.2328)
Nζ@Lys73···Oδ@Asn132	2.82 (0.1660)	2.88 (0.1542)
Nδ@Asn132···O @Asp104	2.92 (0.1721)	2.93 (0.1585)
N@Ser70···O8@SUL	3.03 (0.2631)	2.90 (0.1541)
N@Ala237···O8@SUL	2.88 (0.1347)	2.96 (0.1987)
Ow@Wat···C6@SUL	3.46 (0.2436)	3.31 (0.1682)
Ow@Wat···N4@SUL	3.95 (0.5857)	3.35 (0.3984)
Ow@Wat···O9@SUL	6.38 (0.8094)	6.62 (0.7943)

[a] Values in parentheses is standard deviation (in Å).

Based on the MD trajectory of **imine_WT**, we found that several amino acid residues (Ser70, Ala237, Lys73, Ser130, Glu166, Asn170, Asn132 and Asp104) around the active site formed hydrogen bonds with substrates or with residues each other. Glu166

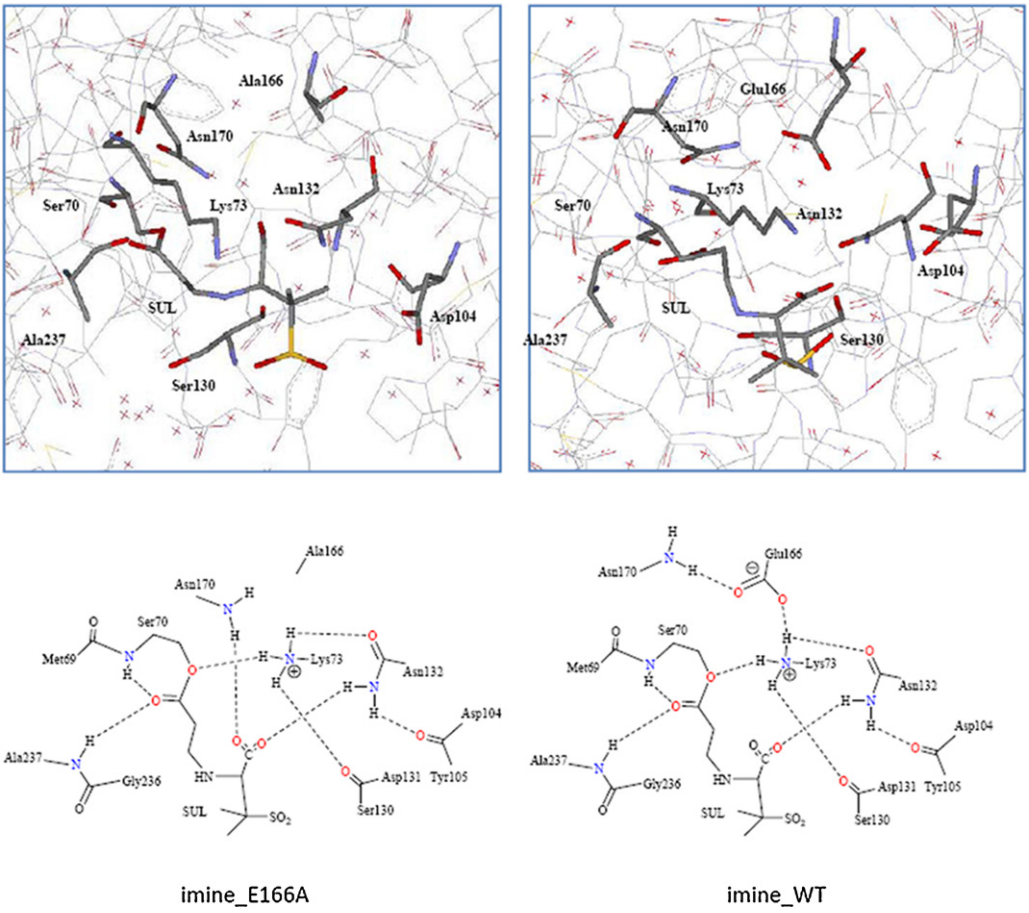

Fig. 2. The hydrogen bond network around active site in **imine_E166A** and **imine_WT**.

is known to be the catalytically important residue [28–31,34]. The distances indicate that Oε1 and Oε2 of the Glu166 make two stable hydrogen bonds with the side chains of Asn170 and Lys73. Besides, the angles also indicate stable hydrogen bonds are made. The average Oε1@Glu166···H—Nδ@Asn132 angle is 145°, and average Oε2@Glu166···H—Nζ@Lys73 angle is 121°. The ammonium group of Lys73 was located on the center of hydrogen bond network, and it forms four hydrogen bonds with Glu166, Ser70, Ser130 and Asn132 respectively. This is consistent with previous reported experimental results [35,36]. The Asn132 made a contact with the backbone carbonyl group of Asp104. Besides, Asn132 also formed hydrogen bond with substrate, and the average distance of O10@SUL···Nδ@Asn132 was 3.18 Å. We have observed one water molecule in the crystal structure at a hydrogen-bond distance of the Lys73-Nζ, Asn132-Oδ and Ser70-Oγ atoms. The conserved water molecule remained in its position in the MD simulations and might be important for the stability of the binding site. The carboxyl oxygen of the sulbactam (O8) was trapped by an "oxyanion hole" that consists of two NH groups of the main chains in Ser70 and Ala237. The distances between SULO8 and Ser70N and SULO8 and Gln237N were observed within the range of the hydrogen bond. The average of the two atomic distances was 2.90 and 2.96 Å. These results indicate that O8 is constrained by the oxyanion hole. It indicates the conformation of oxyanion hole is quite stable, and it plays an important role to stabilize the negative charge on the O8 atom.

The stable "oxyanion hole" was also observed in MD trajectory of **imine_E166A**. Besides, there are Lys73, Ser130, Asn170, Asn132 and Asp104 around the active site of **imine_E166A**. Different from **imine_WT**, the Glutamic acid is replaced by Alanine at 166 position in **imine_E166A**, and Ala166 cannot form hydrogen bond with Asn170 and Lys73. Compared to **imine_WT**, the interaction between Oγ@Ser70···Nζ@Lys73 was not stable in **imine_E166A**, and it fluctuated from 3.1 to 6.9 Å (Fig. 3). The average distance is 4.74 Å, and calculated standard deviation is 0.5210 Å. However, Lys73 forms stable hydrogen bonds with Ser130 and Asn132 respectively, which is similar to **imine_WT**. We also observed the conserved water molecule kept among the Lys73-Nζ, Asn132-Oδ and Ser70-Oγ atoms. However, the average distance of the O@water···Nζ@Lys73 is 4.27 Å which is longer than that of **imine_WT** by 1.15 Å. From MD trajectory of **imine_E166A**, we found that there were two residues (Asn132 and Asn170) around substrate carboxyl. Nδ@Asn170 form stable hydrogen bond with substrate carboxyl, and the average distance Nδ@Asn170···O9@SUL was 2.93 Å. In **imine_WT**, it was not found

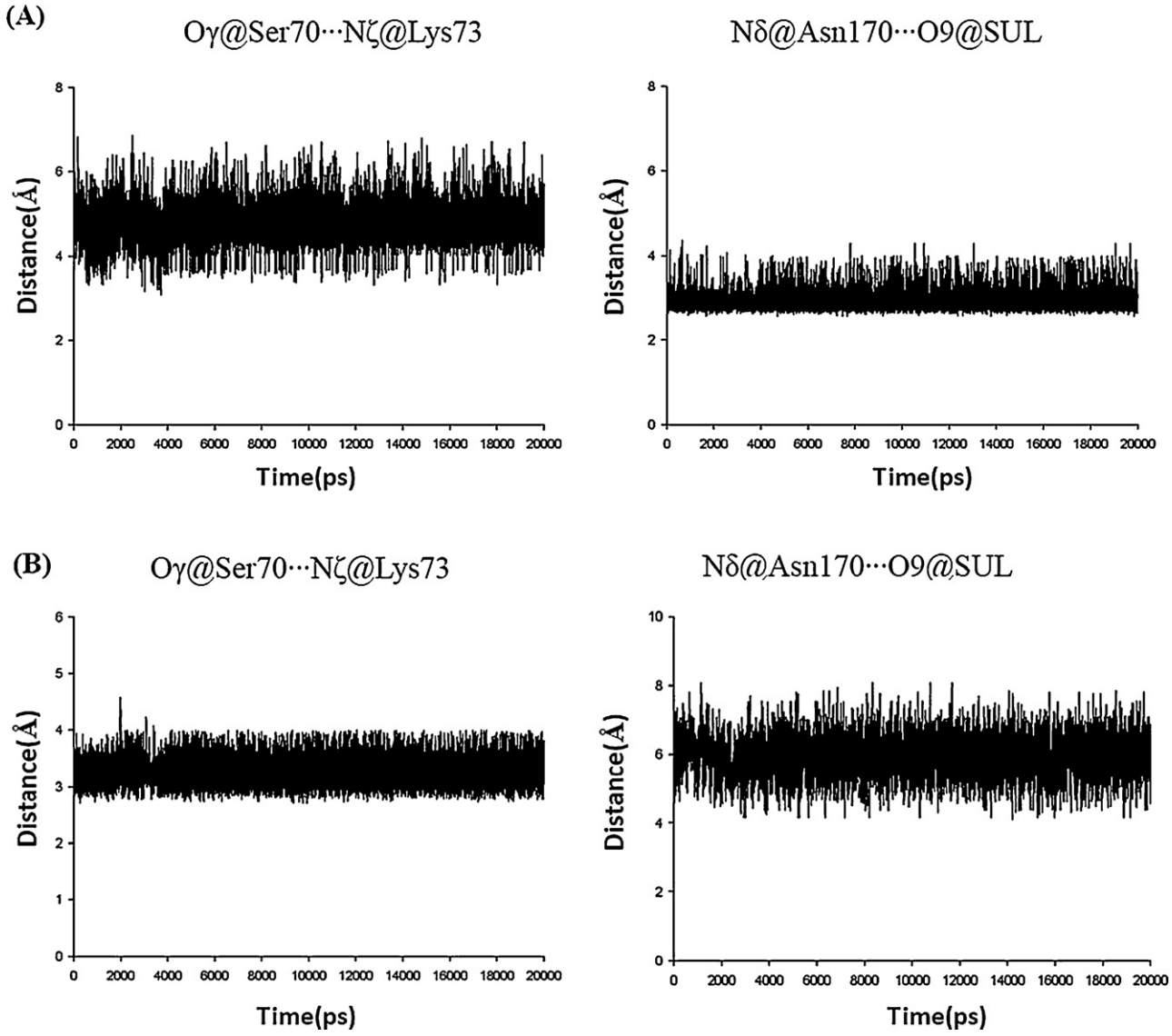

Fig. 3. Distances of Oγ@Ser70···Nζ@Lys73 and Nδ@Asn170···O9@SUL along MD simulations of (A) **imine_E166A** and (B) **imine_WT**.

that the substrate carboxyl has very close contact with Asn170 (Fig. 3). It is obvious that the hydrogen bonds network around active site was changed in E166A because of lacking Glu166.

3.2. The imine substrate conformation in WT and E166A SHV-1

Herein, we focus on the imine intermediate conformation in different protein environment. By checking the conformations along MD trajectories, we found the most significant difference between **imine_WT** and **imine_E166A** involved in the dihedral angle N4—C5—C6—C7 (Fig. 4). In **imine_WT**, the dihedral angle N4—C5—C6—C7 mostly ranges from 60 to 120°, and the average value is 83°. In **imine_E166A**, the dihedral angle N4—C5—C6—C7 is mainly located from −120 to −180°, and the average value is 142°, which represents nearly trans conformation. We have tested the reproducibility of the simulation by performing another 10 ns MD run with different initial velocities. The similar results were obtained (Figure S2 in Supplementary material). By analyzing hydrogen bond network, it was found that Asn170 formed a stable hydrogen bond with carboxyl of substrate. However, such an interaction was not found in **imine_WT**. From **imine_WT** trajectory, it was found that the distance Nδ@Asn170···O9@SUL was large and fluctuated from 4.15 Å to 8.06 Å (Fig. 3). The calculated standard deviation is 0.5532 Å. It suggests that interaction between Asn170 and carboxyl of substrate effect the C5—C6 bond rotation. In **imine_WT**, there exists stable Nδ@Asn170···Oε1@Glu166 interaction (Figure S3 in Supplementary material). It is possible that the Glu166 restrict the Asn170 motion so that Asn170 cannot interact with carboxyl of substrate.

Furthermore, we checked the dihedral angle Nδ—Cγ—Cβ—Cα of Asn170 (Fig. 5). In **imine_E166A**, the dihedral angle Nδ—Cγ—Cβ—Cα mostly ranges from 120° to 160°, and the average value is 144°. It is interesting to note that there is some relation between Nδ—Cγ—Cβ—Cα and the distance Nδ@Asn170···O9@SUL. For example, at ~600 ps, the angle Nδ—Cγ—Cβ—Cα decreased, while the distance Nδ@Asn170···O9@SUL increased (Figs. 3 and 5). In **imine_WT**, the average value of angle Nδ—Cγ—Cβ—Cα is 90°, and most of the values are located from 70° to 100°. It suggests that the Asn170 is trapped by Glu166 in **imine_WT**.

Previous experimental studies have suggested that the imine AEI tautomerizes to yield a more stable cis or trans-enamine intermediates thus provides transient inhibition. Herein, we consider conformation of imine intermediate is a key which determines the subsequent tautomerization. Our results suggest that the distribution of the trans and cis enamine intermediates relate to the dynamic behavior of imine reactant. If the imine represents trans conformation, the trans-enamine can be generated by proton transfer from C5 to N4. On the other hand, if the imine represents cis conformation, a cis-enamine can be generated by proton transfer from C5 to N4. Based on the conformation of imine intermediate in **imine_E166A**, imine intermediate can hardly generate cis conformation because of the interaction between Asn170 and substrate carboxyl. So it can only generate trans enamine intermediate by proton transfer. In contrast, imine in **imine_WT** can generate trans

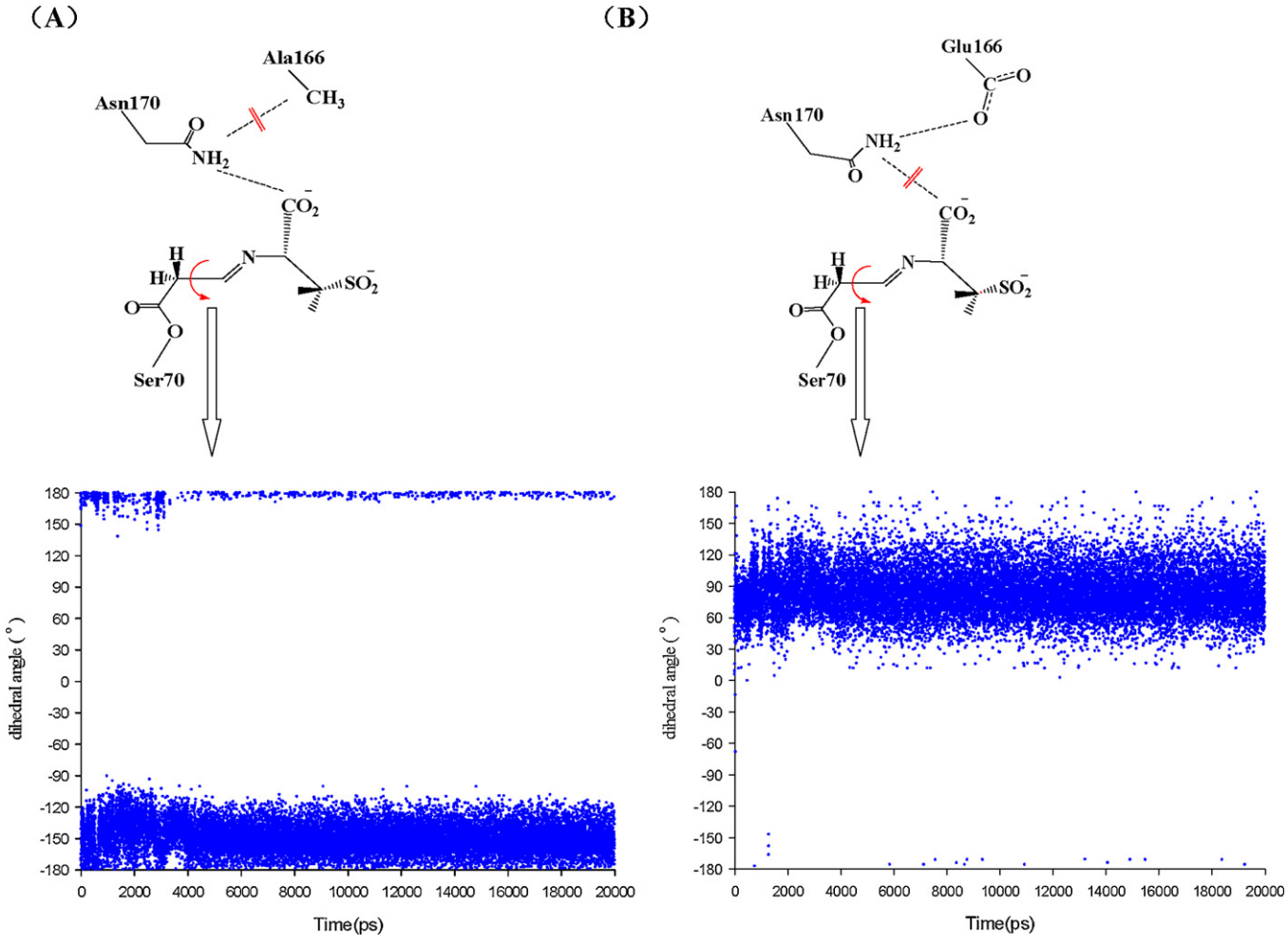

Fig. 4. The distribution of dihedral angle N4—C5—C6—C7 of sulbactam along MD simulations of (A) **imine_E166A** and (B) **imine_WT**.

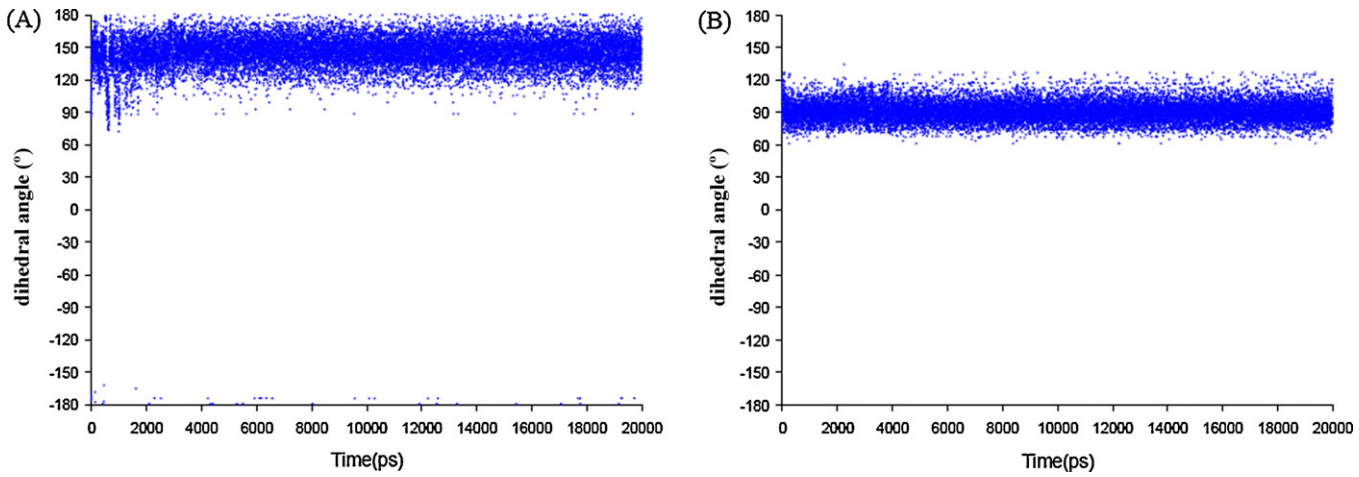

Fig. 5. The distribution of dihedral angle Nδ—Cγ—Cβ—Cα of Asn170 along MD simulations of (A) **imine_E166A** and (B) **imine_WT**.

and cis conformations respectively by C5—C6 rotation, and a mix intermediates population can be obtained.

3.3. The tautomerization from imine to trans-enamine

To further study the tautomerization mechanism from imine to trans-enamine, we performed QM calculations. Herein, the simple QM models were constructed with the residues removed. Ser70 bonding to the sulbactam was truncated and hydrogen atom was added manually. All structures along reaction paths (Fig. 6) were fully optimized at B3LYP/6-31+G* and B3LYP/6-31++G** level respectively. Solvent effects were taken into consideration implicitly through single point calculations on the optimized geometries including the polarized continuum model. Although the solvent effect shift the energy barrier of each step by a few kcal/mol, the basic feature of the potential energy profiles of each step captured from gas phase calculations remains the same. The geometries of each stationary points calculated by B3LYP/6-31+G* and B3LYP/6-31++G** levels are similar. The values of bond lengths, bond angles and dihedrals show tiny discrepancy. The energy barriers computed by B3LYP/6-31++G** were lower than B3LYP/6-31+G* (Table 2). However, both they produce the same conclusions. Herein, we only present the data calculated at B3LYP/6-31++G** level. The geometries of all reactants, transition states and products are shown in Fig. S4 (in Supplementary material).

In the initial reactant **Imine**, the optimized dihedral angle N4—C5—C6—C7 was 177°, and the distance between C6 and N4 was 2.49 Å. This close distance indicated the proton could directly transfer from C6 to N4. We calculated the transition state **TsCN**. In structure of **TsCN**, the dihedral angle N4—C5—C6—C7 became 171°, and the distance of C6-N4 was 2.21 Å. The energy barrier for this process was 42.63 kcal/mol. The energy barriers for direct proton transfer are so high that the reactions are difficult to proceed. However, the water molecule may participate in the reaction. From MD trajectories, we looked for the closest water molecules around

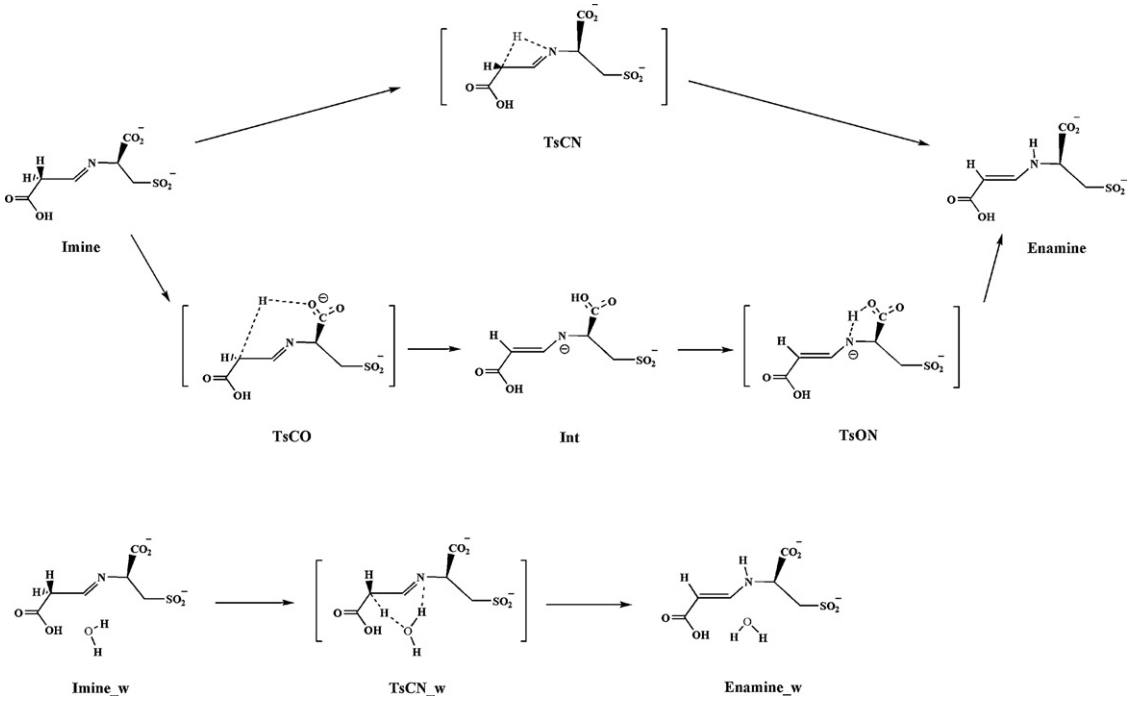

Fig. 6. Reaction paths for QM calculations.

Table 2
Energies of the structures involved in the QM calculations.

	B3lyp/6-31+g*		B3lyp/6-31+g*(PCM)		B3lyp/6-31++g**		B3lyp/6-31++g**(PCM)	
	Total energy[a]	Rel energy[a]	Total energy	Rel energy	Total energy	Rel energy	Total energy	Rel energy
Imine	−1216.22608	0[b]	−1216.31396	0[b]	−1216.25256	0[b]	−1216.33996	0[b]
Enamine	−1216.24494	−11.83	−1216.33065	−10.47	−1216.27335	−13.04	−1216.35856	−11.64
TsCN	−1216.15489	44.67	−1216.24207	45.11	−1216.18462	42.63	−1216.26943	44.25
TsCO	−1216.21653	5.99	−1216.29984	8.86	−1216.24589	4.18	−1216.32893	6.92
Int	−1216.23154	−3.42	−1216.31617	−1.38	−1216.26205	−5.95	−1216.34544	−3.44
TsON	−1216.23033	−2.66	−1216.31485	−0.58	−1216.26122	−5.43	−1216.34356	−2.26
Imine_w	−1292.63782	0[c]	−1292.73144	0[c]	−1292.67483	0[c]	−1292.76763	0[c]
TsCN_w	−1292.60011	23.66	−1292.69199	24.75	−1292.63883	22.59	−1292.72947	23.94
Enamine_w	−1292.65535	−11.00	−1292.74766	−10.18	−1292.69462	−12.42	−−1292.78502	−10.91

[a] Total energy in Hartrees and relative energies in kcal/mol.
[b] In non-water-assisted reactions, the relative energy of **Imine** is 0.
[c] In water-assisted reaction, the relative energy of **Imine_w** is 0.

C6 from every frame. Then the distances C6–Ow, N4–Ow and O9–Ow were measured respectively. The average distances have been included in Table 1, together with their standard deviation values. It suggests that there are stable water molecules between C6 and N4 both in **imine_E166A** and **imine_WT**. They could participate in the proton transfer reactions, namely, the water molecule acts as the bridge of hydrogen transfer. We investigated water-assisted mechanism by QM calculations. The initial reactant is **Imine_w**. In **Imine_w**, the Ow of water is localized around C6 and N4. The distance between Ow and C6 is 2.87 Å, and the distance between Ow and N4 is 3.11 Å. The determined transition state is **TsCN_w**. In the transition state structure, the distance between Ow and C6 becomes 2.55 Å, and the distance between Ow and N4 becomes 2.59 Å. Analysis of imaginary frequency shows that the proton transfers from C6 to O atom of water, and another proton on water molecule transfers to N4 at the same time. The calculated energy barrier for the water-assisted tautomerization is 22.59 kcal/mol. These results indicate the direct proton transfer may be occurred due to the presenting of water as catalyst. Compared with **Imine** and **Imine_w**, the relative energies of **Enamine** and **Enamine_w** are −13.04 and −12.42 kcal/mol respectively, which indicate that the enamine intermediate is more stable than imine.

Besides, we also found a close distance between C6 and O9 in **Imine** (2.92 Å). Thereby we suggest a stepwise proton transfer reaction; viz. the proton transfers from C6 to O9 firstly, followed transfer from O9 to N4. The transition state of first step is **TsCO**. In **TsCO**, distance of C6-O9 becomes 2.78 Å, and the dihedral angle N4—C5—C6—C7 becomes −170°. It indicates that the C5—C6 bond rotations and makes the distance between C6 and O9 decrease in the reaction process. The energy barrier is 4.18 kcal/mol, which is a lot lower than that in C···N proton transfer. The intermediate of the stepwise reaction is **Int**, which is more stable than **Imine**. In **Int**, distance of O9–N4 is 2.39 Å, and the dihedral angle N4—C5—C6—C7 is −179°, which presents a trans conformation. The transition state of the second step is **TsNO**, and the energy barrier is only 0.52 kcal/mol. Compared with direct proton transfer, the stepwise proton transfer involves in very low energy barrier which makes the imine tautomerize to trans-enamine more easily.

However, the MD conformations should be considered to evaluate the rationality of the mechanism. In MD simulations, the conformations were affected by the protein environment which presented a more realistic result. In **imine_E166A**, the close distance between C6 and O9 can be observed (Fig. 7) by analyzing MD trajectory. The average distance is 3.35 Å, and the closest distance is only 2.37 Å. We also checked the distance between O9 and N4, and the average distance is 2.65 Å. These distances are appropriate for stepwise proton transfer. However, the distance between C6 and O9 is elongated in **imine_WT**. The average distance is 4.66 Å, and the closest distance is 3.36 Å. Such distance is unfavorable for the proton transfer. Moreover, there are not stable water molecule observed between C6 and O9 which indicates that the water molecule cannot participate in the reaction (Figure S5 in Supplementary material). It suggests the stepwise proton transfer is hard to proceed in **imine_WT**.

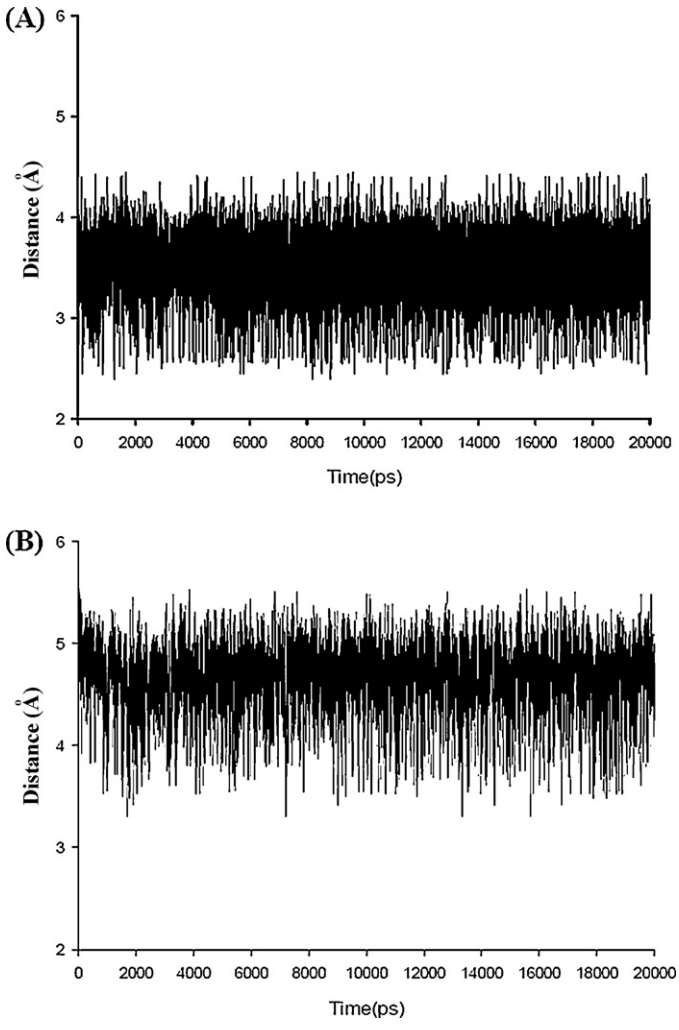

Fig. 7. Distance of C6···O9 in sulbactam along MD simulations of (A) **imine_E166A** and (B) **imine_WT**.

4. Conclusions

In this work, we have investigated the tautomerization mechanism of sulbactam intermediates from imine to trans-enamine in different enzyme including E166A and WT SHV-1 β-lactamases. The following conclusions can be drawn from our study.

In E166A SHV-1 β-lactamase, Asn170 forms stable hydrogen bond with substrate carboxyl, and restricts the C5—C6 bond rotation. Thus the dihedral angle N4—C5—C6—C7 is mainly located around −150° which represents nearly trans conformation. In WT SHV-1 β-lactamase, Asn170 cannot form stable hydrogen bond with substrate carboxyl, because it is trapped by Glu166. Thus the imine C6—C5 bond can rotate freely. Based on the conformation studies of different AEI, we found that imine only generated trans-enamine intermediate in E166A, while generated a mix intermediates in WT. Besides, the interaction between Asn170 and substrate carboxyl led the very close distance of C6···O9. So the substrate carboxyl can participate in the proton transfer reaction acting as a relay station in E166A. The QM calculations showed the stepwise proton transfer had lower energy barrier than direct path, which indicated faster rate of tautomerization from imine intermediate to trans-enamine intermediate in E166A. Our study provided a possible explanation for the corresponding experimental results.

Water plays an important role to assist the proton transfer reactions, and the direct proton transfer may occur due to the presenting of water as catalyst. Compared with the solvent effect, water assistance affects the active energy greatly. Water assistance can shorten the distance of hydrogen migration. Moreover, it would hardly distort the well-balanced structure thus has a relaxed transition state in each process.

We also characterized the role of carboxyl of substrate in inhibiting E166A SHV-1 β-lactamase. First, it can interact with active site residues and stabilize imine intermediate to the trans conformation. Second, it can assist the tautomerization reaction from imine to enamine. It suggests that the carboxyl group of substrate is important for the tautomerization step of the inhibition process. These findings will be potentially useful in the development of new inhibitors.

Appendix A. Supplementary data

Supplementary data associated with this article can be found, in the online version, at http://dx.doi.org/10.1016/j.jmgm.2012.12.002.

References

[1] J.M. Frère, B. Joris, Penicillin-sensitive enzymes in peptidoglycan biosynthesis, Critical Reviews in Microbiology 11 (1985) 299–396.
[2] J. Davies, Inactivation of antibiotics and the dissemination of resistance genes, Science 264 (1994) 375.
[3] K. Bush, G. Jacoby, A. Medeiros, A functional classification scheme for ß-lactamases and its correlation with molecular structure, Antimicrobial Agents and Chemotherapy 39 (1995) 1211–1233.
[4] I. Massova, S. Mobashery, Structural and mechanistic aspects of evolution of beta-lactamases and penicillin-binding proteins, Current Pharmaceutical Design 5 (1998) 929–937.
[5] R.P.A. Brown, R.T. Aplin, C. Schofield, Inhibition of TEM-2 beta-lactamase from *Escherichia coli* by clavulanic acid:observation of intermediates by electrospray-ionization mass-spectrometry, Journal of Biochemistry 35 (1996) 12421–12432.
[6] K. Bush, C. Macalintal, B.A. Rasmussen, V.J. Lee, Y. Yang, Kinetic interactions of tazobactam with beta-lactamases from all major structural classes, Antimicrobial Agents and Chemotherapy 37 (1993) 851–858.
[7] C.C. Chen, O. Herzberg, Inhibition of beta-lactamase by clavulanate: trapped intermediates in cryocrystaliographic studies, Journal of Molecular Biology 224 (1992) 1103–1113.
[8] M.S. Helfand, M.A. Totir, M.P. Carey, A.M. Hujer, R.A. Bonomo, P.R. Carey, Following the reactions of mechanism-based inhibitors with beta-lactamase by raman crystallography, Biochemistry 42 (2003) 13386–13392.
[9] U. Imtiaz, E.M. Billings, J.R. Knox, E.K. Manavathu, S.A. Lerner, S. Mobashery, Inactivation of class A beta-lactamases by clavulanic acid: the role of arginine-244 in a proposed nonconcerted sequence of events, Journal of the American Chemical Society 115 (1993) 4435–4442.
[10] P.S. Padayatti, M.S. Helfand, M.A. Totir, M.P. Carey, P.R. Carey, R.A. Bonomo, F.v.d. Akker, High resolution crystal structures of the trans-enamine intermediates formed by sulbactam and clavulanic acid and E166A SHV-1 beta-lactamase, Journal of Biological Chemistry 280 (2005) 34900–34907.
[11] P.S. Padayatti, M.S. Helfand, M.A. Totir, M.P. Carey, A.M. Hujer, P.R. Carey, R.A. Bonomo, F.v.d. Akker, Tazobactam forms a stoichiometric trans-enamine intermediate in the E166A variant of SHV-1 beta-lactamase: 1.63 Å crystal structure, Biochemistry 43 (2004) 843–848.
[12] D. Sulton, D. Pagan-Rodriguez, X. Zhou, Y. Liu, A.M. Hujer, C.R. Bethel, M.S. Helfand, J.M. Thomson, V.E. Anderson, J.D. Buynak, L.M. Ng, R.A. Bonomo, Clavulanic acid inactivation of SHV-1 and the inhibitor-resistant S130G SHV-1 β-lactamase, Journal of Biological Chemistry 280 (2005) 35528–35536.
[13] P. Swarén, D. Golemi, S. Cabantous, A. Bulychev, L. Maveyraud, S. Mobashery, J.-P. Samama, X-ray structure of the Asn276Asp variant of the escherichia coli TEM-1 β-lactamase:direct observation of electrostatic modulation in resistance to inactivation by clavulanic acid, Biochemistry 38 (1999) 9570–9576.
[14] M.A. Totir, M.S. Helfand, M.P. Carey, A. Sheri, J.D. Buynak, R.A. Bonomo, P.R. Carey, Sulbactam forms only minimal amounts of irreversible acrylate-enzyme with SHV-1 beta-lactamase, Biochemistry 46 (2007) 8980–8987.
[15] M. Kalp, M.A. Totir, J.D. Buynak, P.R. Carey, Different intermediate populations formed by tazobactam, sulbactam, and clavulanate reacting with SHV-1 beta-lactamases: raman crystallographic evidence, Journal of the American Chemical Society 131 (2009) 2338–2347.
[16] D.A. Case, T.A. Darden, I.T.E. Cheatham, C.L. Simmerling, J. Wang, R.E. Duke, R. Luo, M. Crowley, R.C. Walker, W. Zhang, K.M. Merz, B. Wang, S. Hayik, A. Roitberg, G. Seabra, I. Kolossváry, K.F. Wong, F. Paesani, J. Vanicek, X. Wu, S.R. Brozell, T. Steinbrecher, H. Gohlke, L. Yang, C. Tan, J. Mongan, V. Hornak, G. Cui, D.H. Mathews, M.G. Seetin, C. Sagui, V. Babin, P.A. Kollman, AMBER 10, University of California, San Francisco, 2008.
[17] M.J. Frisch, G.W. Trucks, H.B. Schlegel, G.E. Scuseria, M.A. Robb, J.R. Cheeseman, J.A. Montgomery Jr., T.V. Vreven, K.N. Kudin, J.C. Burant, J.M. Millam, S.S. Iyengar, J. Tomasi, V. Barone, B. Mennucci, M. Cossi, G. Scalmani, N. Rega, G.A. Petersson, H. Nakatsuji, M. Hada, M. Ehara, K. Toyota, R. Fukuda, J. Hasegawa, M. Ishida, T. Nakajima, Y. Honda, O. Kitao, H. Nakai, M. Klene, X. Li, J.E. Knox, H.P. Hratchian, J.B. Cross, C. Adamo, J. Jaramillo, R. Gomperts, R.E. Stratmann, O. Yazyev, A.J. Austin, R. Cammi, C. Pomelli, J.W. Ochterski, P.Y. Ayala, K. Morokuma, G.A. Voth, P. Salvador, J.J. Dannenberg, V.G. Zakrzewski, S. Dapprich, A.D. Daniels, M.C. Strain, O. Farkas, D.K. Malick, A.D. Rabuck, K. Raghavachari, J.B. Foresman, J.V. Ortiz, Q. Cui, A.G. Baboul, S. Clifford, J. Cioslowski, B.B. Stefanov, G. Liu, A. Liashenko, P. Piskorz, I. Komaromi, R.L. Martin, D.J. Fox, T. Keith, M.A. Al-Laham, C.Y. Peng, A. Nanayakkara, M. Challacombe, P.M.W. Gill, B. Johnson, W. Chen, M.W. Wong, C. Gonzalez, J.A. Pople, Gaussian03, Gaussian Inc., Pittsburgh, PA, 2003.
[18] J. Wang, P. Cieplak, P.A. Kollman, How well does a restrained electrostatic potential (RESP) model perform in calculating conformational energies of organic and biological molecules, Journal of Computational Chemistry 21 (2000) 1049–1074.
[19] J. Wang, R.M. Wolf, J.W. Caldwell, P.A. Kollamn, D.A. Case, Development and testing of a general amber force field, Journal of Computational Chemistry 25 (2004) 1157–1174.
[20] S.D. Kotsakis, L.S. Tzouvelekis, E. Petinaki, E. Tzelepi, V. Miriagou, Effects of the Val211Gly substitution on molecular dynamics of the CMY-2 cephalosporinase: implications on hydrolysis of expanded-spectrum cephalosporins, Proteins 79 (2011) 3180–3192.
[21] S.O. Meroueh, J.F. Fisher, H.B. Schlegel, S. Mobashery, Ab Initio QM/MM study of class A β-lactamase acylation: Dual participation of Glu166 and Lys73 in a concerted base promotion of Ser70, Journal of the American Chemical Society 127 (2005) 15397–15407.
[22] A. Miani, M.S. Helfand, S. Raugei, Ab initio Raman spectra of β-lactamase inhibitor intermediates bound to E166A SHV β-lactamase, Journal of Chemistry Theory and Computation 5 (2009) 2158–2172.
[23] J.P. Ryckaert, G. Ciccotti, H.J.C.J. Berendsen, Numerical integration of the cartesian equations of motion of a system with constraints: molecular dynamics of n-alkanes, Journal of Computational Physics 23 (1977) 327–341.
[24] R.W. Pastor, B.R. Brooks, A. Szabo, An analysis of the accuracy of langevin and molecular-dynamics algorithms, Molecular Physics 65 (1988) 1409–1419.
[25] V. Essman, L. Perera, M.L. Berkowitz, T. Darden, H. Lee, L.G. Pedersen, A smooth particle-mesh-Ewald method, Journal of Chemical Physics 103 (1995) 8577–8593.
[26] A.D. Becke, Density-functional thermochemistry. III. The role of exact exchange, Journal of Chemical Physics 98 (1993) 5648–5652.
[27] C. Lee, W. Yang, R.G. Parr, Development of the Colle–Salvetti correlation-energy formula into a functional of the electron density, Physical Review B 37 (1988) 785–789.
[28] N. Díaz, T.L. Sordo, J. Kenneth, M. Merz, D. Suárez, Insights into the acylation mechanism of class A beta-lactamases from molecular dynamics simulations of the TEM-1 enzyme complexed with benzylpenicillin, Journal of the American Ceramic Society 125 (2003) 672–684.
[29] N. Díaz, D. Suárez, T.L. Sordo, J. Kenneth, M. Merz, Acylation of Class A beta-lactamases by penicillins: a theoretical examination of the role of Serine 130 and the beta-lactam carboxylate group, Journal of Physical Chemistry B 105 (2001) 11302–11313.

[30] J.C. Hermann, C. Hensen, L. Ridder, A.J. Mulholland, H.-D. Höltje, Mechanisms of antibiotic resistance: QM/MM modeling of the acylation reaction of a class A β-lactamase with benzylpenicillin, Journal of the American Chemical Society 127 (2005) 4454–4465.
[31] J.C. Hermann, L. Ridder, A.J. Mulholland, H.-D. Höltje, Identification of Glu166 as the general base in the acylation reaction of class A beta-lactamases through QM/MM modeling, Journal of the American Chemical Society 125 (2003) 9590–9591.
[32] J. Tomasi, M. Persico, Molecular interactions in solution: an overview of methods based on continous distributions of the solvent, Chemical Reviews 94 (1994) 2027–2094.
[33] C. Gonzalez, H.B. Schlegel, Reaction path following in mass-weighted internal coordinates, Journal of Physical Chemistry B 94 (1990) 5523–5527.
[34] Y. Fujii, N. Okimoto, M. Hata, T. Narumi, K. Yasuoka, R. Susukita, A. Suenaga, N. Futatsugi, T. Koishi, H. Furusawa, A. Kawai, T. Ebisuzaki, S. Neya, T. Hoshino, Molecular dynamics study on class A β-lactamase: hydrogen bond network among the functional groups of penicillin g and side chains of the conserved residues in the active site, Journal of Physical Chemistry B 107 (2003) 10274–10283.
[35] C. Jelsch, L. Mourey, J.M. Masson, J.P. Samama, Crystal structure of escherichia coli TEM1 β-lactamase at 1.8 Å resolution, Proteins 16 (1993) 364–383.
[36] A. Matagne, J. Lamotte-Brasseur, J.M. Frère, The catalytic properties of class A beta-lactamases: efficiency and diversity, Biochemical Journal 330 (1998) 581–598.